

Non-Hermitian multiterminal phase-biased Josephson junctions

Jorge Cayao¹ and Masatoshi Sato²

¹*Department of Physics and Astronomy, Uppsala University, Box 516, S-751 20 Uppsala, Sweden*

²*Center for Gravitational Physics and Quantum Information,
Yukawa Institute for Theoretical Physics, Kyoto University, Kyoto 606-8502, Japan*

(Dated: December 31, 2024)

We study non-Hermitian Josephson junctions formed by multiple superconductors and discover the emergence of exceptional points entirely determined by the interplay of the distinct superconducting phases and non-Hermiticity due to normal reservoirs. In particular, in Josephson junctions with three and four superconductors, we find stable lines and surfaces of exceptional points protected by non-Hermitian topology and highly tuneable by the superconducting phases. We also discover that, in Josephson junctions formed by laterally coupled superconductors, exceptional points can result from hybridized Andreev bound states and lead to the enhancement of supercurrents controlled by dissipation. Our work unveils the potential of multiterminal Josephson junctions for realizing higher dimensional topological non-Hermitian superconducting phenomena.

I. INTRODUCTION

The advent of non-Hermitian (NH) topology has spurred great activity in distinct areas of physics due to its potential for designing states of matter with no Hermitian counterpart [1–3]. The intriguing NH topology stems from spectral degeneracies known as exceptional points (EPs), where eigenvalues and eigenvectors coalesce, giving rise to the concept of point gaps in the complex energy plane as a peculiar effect absent in Hermitian setups [4–6]. While in one-dimension EPs appear at single points, they become exceptional lines and surfaces in higher dimensions, originating surprisingly stable topological phases that otherwise do not exist [7–10].

It is now well-understood that dissipation is the mechanism leading to NH physics [3, 11]. A notable realistic physical scenario for dissipative effects is coupling closed systems to normal reservoirs, which naturally appears in quantum transport [12]. These ideas have recently been explored in superconducting systems, [13–24], with intriguing results reporting Andreev EPs and supercurrents due to the interplay of non-Hermiticity and the Josephson effect in junctions formed by two superconductors having a finite phase difference [25, 26]; see also [27–29]. Although these studies reveal the role of a single superconducting phase difference in NH JJs, the impact of non-Hermiticity on JJs formed by multiple superconductors with distinct phases remains unknown. Having JJs with multiple phases is not only a physical curiosity. Understanding the phases as bandstructure quasi-momenta, in the Hermitian regime it has already enabled the realization of higher dimensional states [30–32], Andreev molecules [33–38], and non-local Josephson transport [39–45]. It is therefore natural to wonder about the role of non-Hermiticity on multiterminal JJs for realizing higher dimensional NH topological phases.

This work investigates NH multiterminal JJs by coupling superconductors with distinct superconducting phases to a normal reservoir; see Fig. 1(a,b). In particular, we focus on two types of multiterminal JJs formed

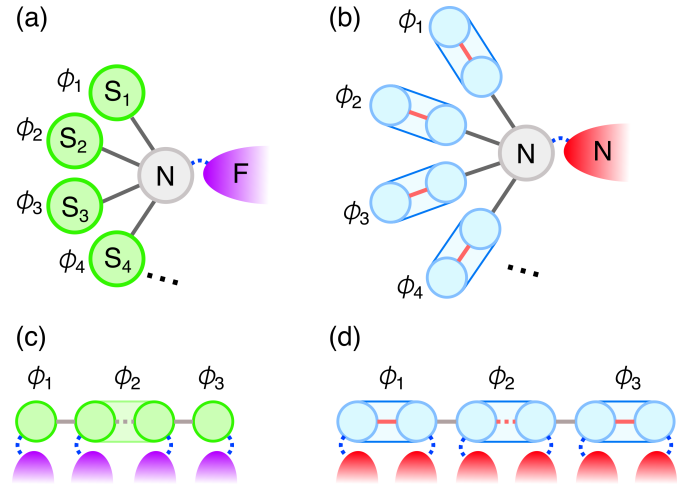


FIG. 1. NH multiterminal JJs. (a) Multiple conventional spin-singlet s -wave superconductors (green, S_i) with distinct phases ϕ_i are coupled to a normal region (gray, N) which is open to a ferromagnetic lead (magenta, F). (b) The same as in (a) but with two-site p -wave superconductors (cyan boxes with linked circles), known as minimal Kitaev chains, coupled to a normal region that is open to a normal reservoir (red, N). (c,d) JJs formed by three superconductors of (a,b), open to ferromagnet and normal reservoirs, respectively.

by conventional spin-singlet s -wave superconductor and minimal Kitaev chains with spin-triplet p -wave superconductivity. We discover that having multiple superconducting phases offers the possibility to realize and control EPs in higher dimensions, originating, for instance, exceptional lines and surfaces connecting stable Fermi arcs in JJs with three and four superconductors. Furthermore, for JJs with laterally coupled superconductors, we find that exceptional points can mediate the formation of hybridized Andreev bound states and produce larger supercurrents that would be tiny otherwise. Our work demonstrates the importance of multiterminal JJs for engineering higher dimensional NH topological phases.

II. NH MULTITERMINAL JJS

We first focus on NH JJs where multiple superconductors (Ss) are coupled to the same normal lead via a quantum dot (N); see Fig. 1(a,b). These open systems are modeled by an effective NH Hamiltonian that reads,

$$H_{\text{eff}}(\phi_i, \omega) = H_{\text{JJ}}(\phi_i) + \Sigma^r(\omega), \quad (1)$$

where $H_{\text{JJ}}(\phi_i)$ models the JJs with superconducting phases ϕ_i and $\Sigma^r(\omega)$ is the frequency-dependent retarded self-energy that accounts for coupling to the lead. Since phase differences matter, when coupling n superconductors, only $n - 1$ phases remain in Eq. (1), which we will exploit when addressing the respective JJs. For pedagogical purposes, we focus on JJs formed by three and four superconductors, including conventional spin-singlet s -wave [46] and minimal Kitaev chains [47, 48] which have spin-triplet p -wave superconductivity [49, 50], see below. The choice of Josephson junctions with distinct number of superconductors is important because it provides an intuitive understanding of the interplay between non-Hermiticity and the multiple superconducting phases for realizing higher dimensional non-Hermitian topological phases. The effective Hamiltonian hosts the particle-hole symmetry, $CH_{\text{eff}}^*(\phi_i, \omega)C^\dagger = -H_{\text{eff}}(\phi_i, -\omega)$, where C is a unitary operator with $CC^* = 1$ [25]. Thus, H_{eff}^* can host topologically stable EPs with zero real energy. Since ϕ_i does not change the sign under particle-hole symmetry, the Hamiltonian belongs to class \mathcal{PD}^\dagger , as demonstrated in the Supplemental Material of Ref. [51]. Thus, from the classification given in Ref. [51], it is very likely that NH multiterminal Josephson junctions will support topologically stable EPs with codimension one, namely EPs in one dimension, exceptional lines in two dimensions, and exceptional surfaces in three dimensions.

A JJ with three superconductors (Ss) is modeled by

$$H_{\text{JJ}} = \begin{pmatrix} H_{S_1} & V^\dagger & 0 & 0 \\ V & H_N & V & V \\ 0 & V^\dagger & H_{S_2} & 0 \\ 0 & V^\dagger & 0 & H_{S_3} \end{pmatrix}, \quad (2)$$

where H_{S_α} and V model the Ss and their coupling to N. A conventional s -wave superconductor S_α is modeled by $H_{S_\alpha}^s = \varepsilon_\alpha \tau_z + \text{Re}(\Delta_\alpha) \sigma_y \tau_y - \text{Im}(\Delta_\alpha) \sigma_y \tau_x$, with an s -wave pair potential $\Delta_\alpha = \Delta e^{i\phi_\alpha}$. Here, σ_i and τ_i are the Pauli matrices in spin and Nambu spaces. Also, $H_N = \varepsilon_N \tau_z$ models the N region, while $V = t\sigma_0 \tau_z$ is the hopping between N and S_α . Non-Hermiticity is considered due to coupling N to a ferromagnet lead F [Fig. 1(a)], which induces a spin-dependent self-energy that in the wide-band limit reads [12, 18, 25] $\Sigma^r(\omega = 0) = \text{diag}(0, \Sigma_N^r, 0, 0)$, with $\Sigma_N^r = \text{diag}(\Sigma_e^r, \Sigma_h^r)$ where $\Sigma_{e,h}^r = -i\Gamma\sigma_0 - i\gamma\sigma_z$, $\Gamma = (\Gamma_\uparrow + \Gamma_\downarrow)/2$, $\gamma = (\Gamma_\uparrow - \Gamma_\downarrow)/2$; Γ_σ is the coupling of spin σ to F. Similarly, we model a NH JJ with four Ss. It is worth noting that, although ferromagnetism and superconductivity might be seen as antagonistic, moderate values of Zeeman fields in the ferromagnet leads are

expected to give sizeable couplings and not to be detrimental [52].

In the case of JJs based on minimal Kitaev chains [Fig. 1(b)], they are modeled by Eq. (2) but with two-site p -wave Ss given by [47, 49] $H_{S_\alpha}^p = \varepsilon_1 \eta_+ \tau_z + \varepsilon_2 \eta_- \tau_z + t_\alpha \eta_x \tau_z + \text{Re}(\Delta_{\alpha_p}) \eta_y \tau_y - \text{Im}(\Delta_{\alpha_p}) \eta_y \tau_x$, where ε_n are the onsite energies, $\Delta_{\alpha_p} = \Delta_\alpha e^{i\phi_\alpha}$ is the p -wave pair potential with phase ϕ_α ; here $\eta_\pm = (\eta_0 \pm \eta_z)/2$ and η_i are Pauli matrices in the site subspace. Moreover, $H_N = \varepsilon_N \tau_z$, while $V = (\tau/2)[\eta_x - i\eta_y, -(\eta_0 - \eta_z)]_{2 \times 4}$. We consider coupling N to a normal lead by $\Sigma_N = -i\Gamma_N$ to account for NH effects. Despite the simplicity of our models, they hold particular experimental relevance in the physics of Andreev molecules [33, 36, 37, 39, 42] and poor man's Majorana modes [53–56]. We are interested in EPs forming in NH JJs given by Eq. (2), especially how the multiple superconducting phases can realize and control them. Since only phase differences matter, we set $\phi_1 = 0$ and numerically explore EPs in the spaces of $\phi_{2,3}$ and $\phi_{2,3,4}$ for three and four terminal JJs, respectively.

A. NH multiterminal JJs based on conventional superconductors

We start by analyzing NH JJs with three and four conventional Ss; see Fig. 2(a,c,e) and Fig. 2(b,d,f), respectively. Fig. 2(a) shows the Re and Im parts of the energy levels for JJs with three Ss as a function of ϕ_2 at $\phi_3 = 0.6\pi$, $\Gamma_\uparrow = 1$, while Fig. 2(b) for JJs with four Ss as a function of ϕ_2 at $\phi_3 = \pi$, $\phi_4 = 0.2\pi$, $\Gamma_\uparrow = 1$. In the Hermitian regime ($\Gamma_\sigma = 0$), the low-energy Andreev spectrum strongly depends on the phases, with the Andreev bound states (ABSs) developing an asymmetric cosine-like profile for $\phi_i = \pi$ that is known to be common in Hermitian multiterminal JJs [31], see gray curves in Fig. 2(a,b). In the NH regime, the lowest positive and negative energy levels, the ABSs, merge at zero Re energy and remain pinned over a finite range of ϕ_2 , see Fig. 2(a,b); within the zero Re energy line (shaded cyan region), the Im parts split but merge at the ends, where we have verified that the associated wavefunctions become parallel. Therefore, since eigenvalues and eigenfunctions coalesce at these points, they are EPs [6], notably, here emerging fully controlled by the multiple superconducting phases of the NH JJs with three and four Ss. The regions with zero Re energy and EPs strongly depend on the interplay of non-Hermiticity and the multiple phases; see insets of Fig. 2(a,b). The fact that non-Hermiticity in Fig. 2(a,b) only affects the ABSs, while maintaining a finite energy gap, is a strong indicator that the superconducting gap is not destroyed.

Further insights on how EPs depend on the phases are obtained from the Re part of the difference between lowest positive and lowest negative energies ($\text{Re}E_{\text{eh}}$), shown in Fig. 2(c,d) as a function of $\phi_{2,3}$ for the spectra in Fig. 2(a,b). The blue regions indicate $\text{Re}E_{\text{eh}} = 0$, which signals the zero Re energy seen in Fig. 2(a,b),

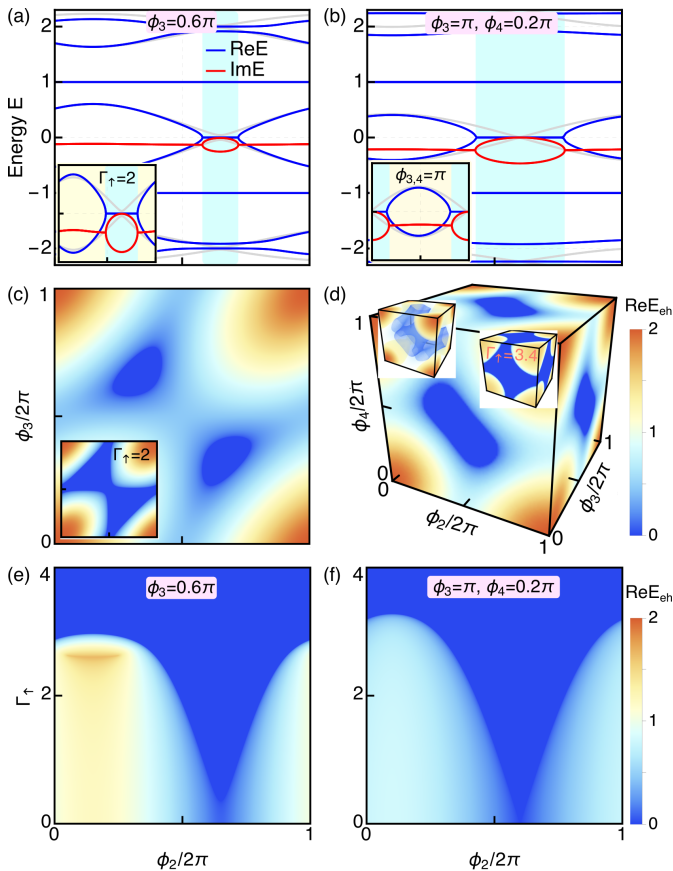


FIG. 2. (a) Re (blue) and Im (red) parts of the eigenvalues of an NH JJ formed by three conventional Ss as a function of ϕ_2 at $\phi_3 = 0.6\pi$, $\Gamma_\uparrow = 1$. The inset shows the same as (a) but for $\Gamma_\uparrow = 2$. (b) The same as in (a) but for a JJ with four conventional superconductors at $\phi_3 = \pi$, $\phi_4 = 0.2\pi$, $\Gamma_\uparrow = 2$. The inset shows the same as (b) but for $\phi_{3,4} = \pi$. The ends of the cyan regions in (a,b) mark the EPs. (c,d) Re part of the difference between the lowest positive and lowest negative eigenvalues of (a,b) as a function of $\phi_{2,3}$ and $\phi_{2,3,4}$. The insets in (c,d) are for $\Gamma_\uparrow = 2$ and $\Gamma_\uparrow = 3.4$, respectively; the left inset in (d) shows the inner side of the blue region. (e,f) Same as in (c,d) as a function of ϕ_2 and Γ_\uparrow for the phases of (a,b). The ends of the blue regions mark the EPs. Parameters: $\phi_1 = 0$, $\Delta = 1$, $t = 1$, $\varepsilon_\alpha = 0$, $\Gamma_\downarrow = 0$.

and their ends mark the EPs. At weak non-Hermiticity [Fig. 2(c,d)], the system does not host EPs at $\phi_{2(3)} = 0$ and $\phi_{2(3,4)} = 0$. Notably, by sweeping all phases ϕ_α from 0 to 2π , we find isolated zero Re energy regions ($\text{Re}E_{\text{eh}} = 0$) with EPs requiring the combined effect of all ϕ_α , see Fig. 2(c,d). The blue area showing $\text{Re}E_{\text{eh}} = 0$ in Fig. 2(c) is a 2D surface with its boundary being a 1D line of EPs (exceptional line), while $\text{Re}E_{\text{eh}} = 0$ in Fig. 2(d) is a 3D volume with its surface being a 2D region of EPs (exceptional surface). As non-Hermiticity increases, the isolated blue EP regions merge along $\phi_2 = -\phi_3$ and also extend to $\phi_{2(3)} = 0$ and $\phi_{2(3,4)} = 0$, see insets of Fig. 2(c,d). The key role of the multiple phases is seen by noting that the blue region with EPs at $\phi_\alpha = 0$ con-

siderably enlarges as the other phases take finite values. To avoid confusion, we note that the blue regions in the faces of the cube in Fig. 2(d) correspond to 2D regions with $\text{Re}E_{\text{eh}} = 0$ which are connected and hence form a 3D volume with $\text{Re}E_{\text{eh}} = 0$. This connection is depicted in the left inset where we show the skeleton of the right inset which represents the exceptional surface of the 3D volume. We thus find that the blue regions in three-terminal JJs reveal exceptional lines of EPs [Fig. 2(c)], while in four terminal JJs we obtain exceptional surfaces [Fig. 2(d)]. Another interesting feature is that having multiple phases at strong non-Hermiticity gives larger regions of $\text{Re}E_{\text{eh}} = 0$ along certain axes in the phase space, see axis $\phi_2 = -\phi_3$ in the inset of Fig. 2(c). The tunability of EPs can be also seen in Fig. 2(e,f), where we present $\text{Re}E_{\text{eh}}$ as a function of Γ_\uparrow and ϕ_2 for the spectra of Fig. 2(a,b). Although not presented, we also emphasize that the onsite energies of the Ss can be useful parameters for controlling the formation of EPs [18, 20]. For realistic conditions, superconductors are large and scalar disorder might be unavoidable; here, scalar disorder modifies the onsite energies, which would then affect the location of the obtained EPs or even allow for EPs due to the interplay of disorder, non-Hermiticity, and the Josephson effect.

B. NH multiterminal JJs based on minimal Kitaev chains

For NH JJs with minimal Kitaev chains, we distinguish two relevant cases: i) $\Delta = t$, $\varepsilon_\alpha = 0$, and ii) $\Delta \neq t$, $\varepsilon_\alpha \neq 0$, both of particular relevance in experiments addressing few-site Kitaev chains [53–56]. For $\Delta = t$ and $\varepsilon_\alpha = 0$, the system hosts poor man’s Majorana modes in the Hermitian regime [47], which are zero energy Majorana modes but without any Hermitian topological protection. For $\Delta \neq t$ and $\varepsilon_\alpha \neq 0$, the system does not host Majorana-like quasiparticles in the Hermitian regime but it can under the influence of non-Hermiticity, recently shown for a NH minimal Kitaev chain [48]. Fig. 3(a,b) shows the Re and Im parts of the energy levels of JJs with three and four Ss as a function of ϕ_2 for finite non-Hermiticity and finite values of ϕ_α at $\Delta \neq t$, $\varepsilon_\alpha \neq 0$. The insets of (a,b) show the Re and Im parts of the energy levels for the respective JJs at $\Delta = t$, $\varepsilon_\alpha = 0$; here, the shown Im parts correspond the energy levels that exhibit EPs. The first observation is that non-Hermiticity induces regions with zero Re energy and split Im parts, whose ends mark EPs in JJs with three and four Ss irrespective of Δ being equal to t or not; see ends of cyan regions in Fig. 3(a,b). For $\Delta \neq t$, EPs form between the lowest positive and lowest negative energies, while EPs at $\Delta = t$ form between first positive/negative excited levels. In both cases, the Re parts develop a circular-like profile between EPs around $\phi_2 = \pi$, while the Im parts stick to the same value between EPs. It is worth noting that EPs between first excited levels at $\Delta = t$ emerge because in

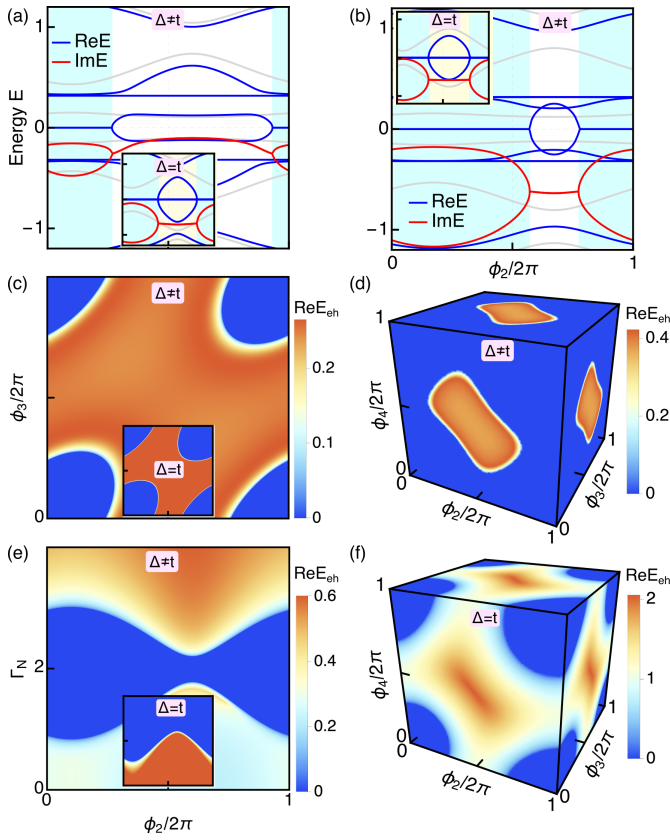


FIG. 3. (a) Re (blue) and Im (red) parts of the eigenvalues of a NH JJ formed by three minimal Kitaev chains as a function of ϕ_2 at $\Delta = 1$, $t = \tau = 0.8$, $\phi_3 = 0.4\pi$, $\Gamma_N = 1$, $\varepsilon_\alpha = 0.5$. (b) Same as in (a) but for a JJ with four minimal Kitaev chains at $\Gamma_N = 2$, $\varepsilon_\alpha = 0.5$, $\phi_3 = 0.6\pi$, $\phi_4 = 0.4\pi$. The insets in (a) and (b) show the same as (a) and (b) but for $\phi_3 = 0.4\pi$ and $\phi_{3,4} = 0.2\pi$, both cases at $\Delta = t = \tau = 1$, $\Gamma_N = 2$, $\varepsilon_\alpha = 0$. The ends of the cyan regions in (a,b) mark the EPs. (c) Re part of the difference between the lowest positive and lowest negative eigenvalues of (a) as a function of $\phi_{2,3}$ at the parameters of (b). The inset shows the same, but for the first excited positive and negative energy levels at the parameters of the inset in (a). (d) The same as (c) for the eigenvalues of (b) as a function of $\phi_{2,3,4}$. (e) The same quantity of (c) as a function of ϕ_2 and Γ_N for the energies of (a). (f) Same as (d) for the first excited positive and negative energy levels, with the parameters of the inset in (b). The blue areas in (c-f) show levels with zero Re energy whose ends mark the EPs. Parameters: $\phi_1 = 0$, $\Gamma_\downarrow = 0$, $t_\alpha = t$.

this case the lowest Re energies corresponding to the poor mans Majorana modes remain at zero [47], depicted by the blue flat line in the insets of Fig. 3(a,b); their Im parts are finite but not shown here. For this reason, the immediate effect of non-Hermiticity at $\Delta = t$ is on the first excited energy levels, which are the ones exhibiting EPs at zero Re energy and protected by NH topology. Since minimal Kitaev chains are small systems, it is unlikely that scalar disorder plays an important role. However, if disorder occurs, additional ingap states might emerge, which can acquire a phase dependence and then develop

EPs.

The tunability of EPs by the interplay of non-Hermiticity and the distinct phases in NH JJs with minimal Kitaev chains can be further seen in Fig. 3(c-f), where we plot the Re part of the difference between levels undergoing EP transitions; the blue regions here indicates having zero Re energy levels with their ends marking EPs. Unlike the EPs in NH JJs with conventional Ss [Fig. 2], here we find that the lowest (first excited) levels closer to $\phi_\alpha = 0$ are more susceptible to become zero energy and form EPs in an asymmetric fashion with respect to e. g., $\phi_2 = \pi$ in Fig. 3(a-d,f). In NH JJs with three Ss [Fig. 3(a,c,e)], the ends of the blue regions mark lines of EPs in the space of $\phi_{2,3}$, while with four Ss such lines become exceptional surfaces as a function of $\phi_{2,3,4}$ [Fig. 3(b,d,f)]. As noted for JJs with four conventional Ss [Fig. 2(d)], the blue regions in the faces of the cube in Fig. 3(d,f)(d,f) are connected and therefore form a 3D volume of zero Re energy; the surface of such volume is a 2D region of EPs or exceptional surface.

We can, therefore, conclude that the interplay of non-Hermiticity and the multiple superconducting phases in multiterminal JJs enables the realization of higher dimensional exceptional regions protected by NH topology with particle-hole symmetry [51].

III. NH JJS WITH THREE LATERALLY COUPLED SS

Having shown the formation of exceptional lines and surfaces in three and four multiterminal JJs, we now analyze NH JJs with laterally coupled Ss and connected to leads as in Fig. 1(c,d). These JJs are of experimental relevance in the context of Andreev molecules [33, 36, 37] and non-local Josephson effect [41–43]. We model these JJs by

$$H_{JJ} = \begin{pmatrix} H_{S_1} & V_{12} & 0 \\ V_{12}^\dagger & H_{S_2} & V_{23} \\ 0 & V_{23}^\dagger & H_{S_3} \end{pmatrix}, \quad (3)$$

where H_{S_α} represents either conventional Ss or minimal Kitaev chains given below Eq. (2), while V_{ij} is the coupling between Ss. Since the length of the middle S has shown to be important for assessing Andreev molecules in conventional Ss [39], for conventional Ss, we consider that H_{S_2} is composed of two sites coupled by $V = \tau\sigma_0\tau_z$: small and large values of τ then model long and short middle S. Also, $V_{12(23)} = t\sigma_0\tau_z$. Non-Hermiticity appears by coupling each S to leads [Fig. 1(c)], such that a self-energy is added to each H_{S_α} in Eq. (3). The self-energy for conventional Ss is $\Sigma^r(\omega = 0) = \text{diag}(\Sigma_1, \Sigma_2, \Sigma_3)$, with $\Sigma_\alpha = \text{diag}(\Sigma_\alpha^e, \Sigma_\alpha^h)$ and $\Sigma_\alpha^{e(h)} = -i\Gamma_\alpha\sigma_0 - i\gamma^\alpha\sigma_z$, $\Gamma_\alpha = (\Gamma_\uparrow^\alpha + \Gamma_\downarrow^\alpha)/2$, $\gamma^\alpha = (\Gamma_\uparrow^\alpha - \Gamma_\downarrow^\alpha)/2$. For JJs in Eq. (3) with minimal Kitaev chains, the couplings are given by $V_{ij}^\dagger = t_{ij}(\eta_x - i\eta_y)\tau_z$; the self-energy has the same structure as for conventional Ss but in terms of

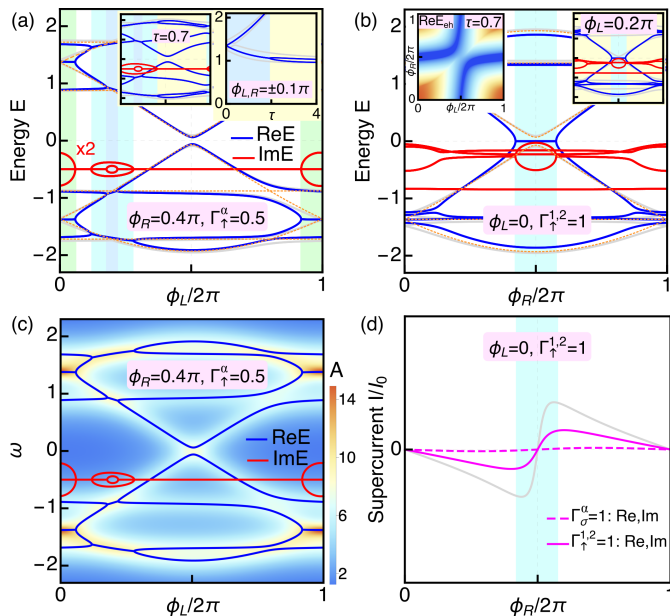


FIG. 4. (a) Re (blue) and Im (red) energy levels as a function of ϕ_L for a JJ with three laterally coupled conventional Ss at $\Gamma_\uparrow^\alpha = 0.5$, $\phi_R = 0.4\pi$, $\tau = 0.3$, while (b) at $\Gamma_\uparrow^{1,2} = 1$, $\Gamma_\uparrow^3 = 0$, $\phi_L = 0$, $\tau = 0.3$. Gray curves correspond to the Hermitian regime at the respective τ , while orange dashed curves depict the Hermitian energies with $\tau = 0$. The left inset in (a) shows the same but for $\tau = 0.7$, while the right inset shows the positive energies as a function of τ at $\phi_{L,R} = 0.1\pi$. The left inset in (b) is the Re energy difference between the lowest positive and the lowest negative energies as a function of $\phi_{L,R}$ at $\tau = 0.7$; the right inset shows the Re and Im energies at $\phi_L = 0.2\pi$. In (a,b), the ends of green, cyan, and blue regions mark the EPs. (c) Spectral function as a function of ω and ϕ_L for the regime of (b). (d) Supercurrents as a function of ϕ_R at $\phi_L = 0$ and $\tau = 0.3$ for distinct values of non-Hermiticity Γ_\uparrow^α , with (solid magenta) and without (dashed magenta) EPs; without EPs we set $\Gamma_\uparrow^\alpha = 1$. Parameters: $\phi_{L(R)} = \phi_{1(3)}$, $\phi_2 = 0$, $\Gamma_\downarrow^\alpha = 0$, $\Delta = 1$, $t = 0.93$, $\varepsilon_S = 0$.

η_i Pauli matrices instead of σ_i and Γ_n^α instead of Γ_σ^α , with $n = 1, 2$ denoting the two sites and α labels the left (L), middle (M), and right (R) Ss. By gauge invariance, we take the phase of H_{S_2} to be zero, $\phi_2 = 0$, and denote $\phi_{1(3)} = \phi_{L/R}$ as the phases of the left and right Ss.

A. NH JJs with three laterally coupled conventional superconductors

We begin by analyzing the NH JJ with three laterally coupled conventional Ss, whose Re and Im energies as a function of ϕ_L are plotted in Fig. 4(a) at $\phi_R = 0.4\pi$, $\tau = 0.3$ and finite non-Hermiticity. In the Hermitian regime ($\Gamma_\sigma^\alpha = 0$) and with $\tau = 0$, the system is composed of two separate JJs: the Andreev spectrum dispersing with ϕ_L corresponds to the left JJ, while the dispersionless levels around $E = \pm 1$ come from the right

JJ, see orange dashed curves in Fig. 4(a). For $\tau = 0.3$, the ABSs hybridize and give rise to an avoided crossing at $\phi_L = \pm\phi_R$ that originating the formation of a Hermitian Andreev molecule [39], see gray curves. A finite non-Hermiticity of the form $\Gamma_\uparrow^\alpha = 0.5$ induces EPs in the Andreev spectrum, which occurs at finite energies between two levels of the same JJ but, notably, also between two levels of distinct JJs. The EPs between levels of the same JJ appear at the ends of the green shaded region in Fig. 4(a), where the Re parts merge within EPs while the Im parts split. The ends of the cyan and blueish regions mark the EPs between levels of distinct JJs. The EPs between levels of the same JJ can be removed by increasing τ but remain robust the EPs between levels of distinct JJs, see left inset of Fig. 4(a). The effect of τ can be further elucidated in the right inset of Fig. 4(a), where we plot the positive energies as a function of τ at $\phi_{L/R} = \pm 0.1\pi$, showing that EPs form between levels of distinct JJs. An interesting consequence of the EPs found here is that they produce large spectral weights, as obtained in the spectral function in the middle S in Fig. 4(c); the lines connecting EPs produce significant spectral features. Therefore, non-Hermiticity can induce and control the formation of Andreev molecules in JJs with conventional Ss beyond the Hermitian regime.

EPs at zero Re energy are possible by taking another choice of non-Hermiticity. This happens, for instance, when introducing the site-dependent ferromagnetic dissipation $\Gamma_\uparrow^{1,2} = 1$ and $\Gamma_\uparrow^3 = 0$, $\Gamma_\downarrow^\alpha = 0$, with the Re and Im energies plotted in Fig. 4(b) as a function of ϕ_R at $\phi_L = 0$. The ends of the cyan region mark such EPs that occur between the lowest positive and negative energy levels. Notably, these levels correspond to already hybridized ABSs of distinct JJs. We have verified that these EPs are highly tunable by $\phi_{L/R}$, reflecting the combined effect of non-Hermiticity and the multiple phases; see left and right insets of Fig. 4(b).

Significantly, these EPs at zero Re energy enhance the Josephson current [25]: Each ABS with quasi-energy E_n carries the supercurrent $I = (-e/\hbar)d\text{Re}E_n/d\phi_L$, which diverges at the EPs. Whereas the Im energy softens the divergence [27–29], the current still exhibits the enhancement. Figure 4(d) shows the supercurrent $I = (-e\hbar/\pi)\text{Im}\sum_n d[E_n \ln(E_n)]/d\phi_L$ [27–29], which includes the softening effect. For comparison, we also plot the current for the system with site- and spin-independent dissipation (dashed curve), which does not host EPs. Although the current with EPs (solid magenta curve) is less than the corresponding Hermitian case without dissipation (gray curve), it is much larger than the current without EPs because of the EPs.

B. NH JJs with three laterally coupled minimal Kitaev chains

Regarding JJs with laterally coupled Kitaev chains, the interplay of non-Hermiticity and $\phi_{L/R}$ provides a con-

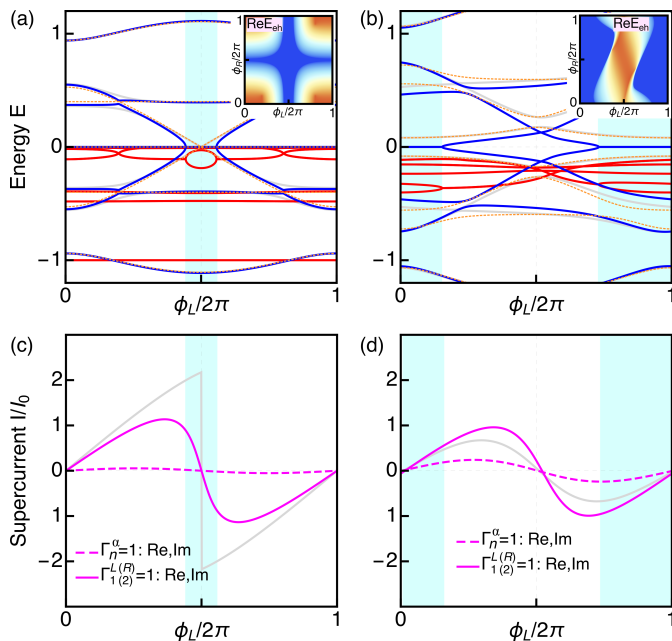


FIG. 5. (a) Re (red) and Im (red) energy levels as a function of ϕ_L for a JJ with three laterally coupled minimal Kitaev chains at $\Gamma_{1(2)}^{L(R)} = 1$, $\phi_R = 0.2\pi$, $t_{1,3} = \Delta_{1,3} = 1$, $t_2 = \Delta_2 = 0.3$, while (b) at $\Gamma_{1(2)}^{L(R)} = 0.5$, $\phi_R = 0.2\pi$, $t_{1,3} = 0.6$, $\Delta_{1,3} = 1$, $t_2 = 0.6$, $\Delta_2 = 0.3$. The gray curves correspond to the Hermitian regime at the respective parameters, while orange dashed curves represent the Hermitian energies at $\phi_R = 0$. The insets show the Re energy difference between the lowest positive and the lowest negative energies as a function of $\phi_{L,R}$. The ends of the cyan and blue regions mark the EPs. (c,d) Supercurrents as a function of ϕ_L for (a,b), with (solid magenta) and without (dashed magenta) EPs; without EPs we set $\Gamma_n^\alpha = 1$. Parameters: $\phi_{L(R)} = \phi_{1(3)}$, $\phi_2 = 0$, $\Gamma_{2(1)}^{L(R)} = 0$, $\Gamma_n^M = 0$, $\Delta = 1$, $t_2 = \tau$, $t_{12} = 0.94$, $t_{23} = 0.4$, $\varepsilon_\alpha = 0$.

trollable way to induce EPs between hybridized ABSs. For instance, in Fig. 5(a) we show the Re and Im energies as a function of ϕ_L at ϕ_R , $t_2 = 0.3$, and $\Gamma_{1(2)}^{L(R)} = 1$ when the Hermitian regime hosts poor man's Majorana modes, seen as lines at zero Re energy. Here, EPs emerge at the ends of the cyan region due to the coalescence at zero Re energy of the first excited positive and negative ABSs, which contain branches from the left and right JJs and can, therefore, be seen as hybridized ABSs or Andreev molecules. The hybridized nature of these NH ABSs can be indeed seen in the orange and gray curves of Fig. 5(a), where we show how the ABSs at $t_2 = 0$ and $t_2 = 0.3$ appear in the Hermitian regime. EPs can also be induced in the absence of Hermitian poor man's Majorana modes, as we indeed show in Fig. 5(b) for $\Gamma_{1(2)}^{L(R)} = 0.5$ and $t_2 = 0.6$.

EPs form between the lowest positive and negative hybridized ABSs at zero Re energy and are marked by the ends of the cyan regions in Fig. 5(b). In both cases of Fig. 5(a,b), the emergence of EPs is an effect highly controllable by the interplay of non-Hermiticity and $\phi_{L,R}$, as demonstrated in the respective insets.

Like the NH JJ with three laterally coupled Ss, the EPs at zero Re energy enhance the Josephson current, as shown in Figs. 5 (c,d). Remarkably, the enhanced current can be more significant than the corresponding Hermitian case. See Fig. 5 (d). Thus, controlling dissipation produces a measurable, otherwise absent positive impact.

IV. CONCLUSIONS

In conclusion, we study non-Hermitian multiterminal phase-biased Josephson junctions. We demonstrate the formation of exceptional points entirely controlled by the interplay of non-Hermiticity and multiple superconducting phases. In particular, for Josephson junctions with three and four superconductors, we discover that exceptional points emerge along lines and surfaces as a highly controllable robust effect protected by NH topology. Furthermore, we show that exceptional points can result from hybridized Andreev bound states of distinct Josephson junctions, enhancing spectral signatures and supercurrents. Our findings are within experimental reach because Josephson junctions similar to the considered here have already been fabricated for studying Andreev molecules [33, 36, 37, 39], the Josephson effect [40–43, 57–59], and poor man's Majorana modes in few-site Kitaev chains [53–56]. Our work paves the way for engineering higher dimensional non-Hermitian topological phenomena controlled by the Josephson effect and non-Hermitian topology.

Note added. Recently, a preprint was posted online (Ref. [60]), which partially overlaps with some of our results.

V. ACKNOWLEDGEMENTS

J. C. acknowledges financial support from the Swedish Research Council (Vetenskapsrådet Grant No. 2021-04121), the Royal Swedish Academy of Sciences (Grant No. PH2022-0003), and the Carl Trygger's Foundation (Grant No. 22: 2093). M. S. was supported by JST CREST Grant No. JPMJCR19T2 and JSPS KAKENHI Grant No. JP24K00569. The computations were enabled by resources provided by the National Academic Infrastructure for Supercomputing in Sweden (NAISS), partially funded by the Swedish Research Council through grant agreement no. 2022-06725

[1] R. El-Ganainy, K. G. Makris, M. Khajavikhan, Z. H. Musslimani, S. Rotter, and D. N. Christodoulides, Non-

Hermitian physics and PT symmetry, Nat. Phys. **14**, 11

- (2018).
- [2] Ş. K. Özdemir, S. Rotter, F. Nori, and L. Yang, Parity–time symmetry and exceptional points in photonics, *Nat. Mater.* **18**, 783 (2019).
 - [3] Y. Ashida, Z. Gong, and M. Ueda, Non-Hermitian physics, *Adv. Phys.* **69**, 249 (2020).
 - [4] Z. Gong, Y. Ashida, K. Kawabata, K. Takasan, S. Higashikawa, and M. Ueda, Topological phases of non-Hermitian systems, *Phys. Rev. X* **8**, 031079 (2018).
 - [5] K. Kawabata, K. Shiozaki, M. Ueda, and M. Sato, Symmetry and topology in non-hermitian physics, *Phys. Rev. X* **9**, 041015 (2019).
 - [6] N. Okuma and M. Sato, Non-Hermitian topological phenomena: a review, *Annu. Rev. Condens. Matter Phys.* , 83 (2023).
 - [7] J. Wiersig, Review of exceptional point-based sensors, *Photonics Res.* **8**, 1457 (2020).
 - [8] M. Parto, Y. G. Liu, B. Bahari, M. Khajavikhan, and D. N. Christodoulides, Non-Hermitian and topological photonics: optics at an exceptional point, *Nanophotonics* **10**, 403 (2020).
 - [9] E. J. Bergholtz, J. C. Budich, and F. K. Kunst, Exceptional topology of non-Hermitian systems, *Rev. Mod. Phys.* **93**, 015005 (2021).
 - [10] T. Bessho, K. Kawabata, and M. Sato, Topological classification of non-Hermitian gapless phases: Exceptional points and bulk fermi arcs, in *Proc. Int. Conf. on Strongly Correlated Electron Systems (SCES2019)* (Physical Society of Japan, 2019) Chap. 30, p. 011098.
 - [11] V. Meden, L. Grunwald, and D. M. Kennes, \mathcal{PT} -symmetric, non-Hermitian quantum many-body physics—a methodological perspective, *Rep. Prog. Phys.* **86**, 124501 (2023).
 - [12] S. Datta, *Electronic transport in mesoscopic systems* (Cambridge university press, 1997).
 - [13] D. I. Pikulin and Y. V. Nazarov, Topological properties of superconducting junctions, *JETP Lett.* **94**, 693 (2012).
 - [14] D. I. Pikulin and Y. V. Nazarov, Two types of topological transitions in finite Majorana wires, *Phys. Rev. B* **87**, 235421 (2013).
 - [15] P. A. Iosevich and M. V. Feigel’man, Tunneling conductance due to a discrete spectrum of Andreev states, *New J. Phys.* **15**, 055011 (2013).
 - [16] P. San-José, J. Cayao, E. Prada, and R. Aguado, Majorana bound states from exceptional points in non-topological superconductors, *Sci. Rep.* **6**, 21427 (2016).
 - [17] J. Avila, F. Peñaranda, E. Prada, P. San-Jose, and R. Aguado, Non-Hermitian topology as a unifying framework for the Andreev versus Majorana states controversy, *Commun. Phys.* **2**, 133 (2019).
 - [18] J. Cayao and A. M. Black-Schaffer, Exceptional odd-frequency pairing in non-Hermitian superconducting systems, *Phys. Rev. B* **105**, 094502 (2022).
 - [19] M. A. Javed, J. Schwibbert, and R.-P. Riwar, Fractional Josephson effect versus fractional charge in superconducting–normal metal hybrid circuits, *Phys. Rev. B* **107**, 035408 (2023).
 - [20] J. Cayao and A. M. Black-Schaffer, Bulk Bogoliubov Fermi arcs in non-Hermitian superconducting systems, *Phys. Rev. B* **107**, 104515 (2023).
 - [21] V. Kornich and B. Trauzettel, Signature of \mathcal{PT} -symmetric non-Hermitian superconductivity in angle-resolved photoelectron fluctuation spectroscopy, *Phys. Rev. Research* **4**, L022018 (2022).
 - [22] R. Mélin, Multiterminal ballistic Josephson junctions coupled to normal leads, *Phys. Rev. B* **105**, 155418 (2022).
 - [23] J. Cayao, Non-Hermitian zero-energy pinning of Andreev and Majorana bound states in superconductor–semiconductor systems, *Phys. Rev. B* **110**, 085414 (2024).
 - [24] M. Ezawa, Even-odd effect on robustness of Majorana edge states in short Kitaev chains, *Phys. Rev. B* **109**, L161404 (2024).
 - [25] J. Cayao and M. Sato, Non-Hermitian phase-biased Josephson junctions, *Phys. Rev. B* **110**, L201403 (2024).
 - [26] C.-A. Li, H.-P. Sun, and B. Trauzettel, Anomalous Andreev bound states in non-Hermitian Josephson junctions, *arXiv:2307.04789* (2023).
 - [27] P.-X. Shen, Z. Lu, J. L. Lado, and M. Trif, Non-Hermitian persistent current transport, *arXiv:2403.09569* (2024).
 - [28] C. W. J. Beenakker, Josephson effect in a junction coupled to an electron reservoir, *arXiv:2404.13976* (2024).
 - [29] D. M. Pino, Y. Meir, and R. Aguado, Thermodynamics of non-Hermitian Josephson junctions with exceptional points, *arXiv:2405.02387* (2024).
 - [30] T. Yokoyama and Y. V. Nazarov, Singularities in the Andreev spectrum of a multiterminal Josephson junction, *Phys. Rev. B* **92**, 155437 (2015).
 - [31] R.-P. Riwar, M. Houzet, J. S. Meyer, and Y. V. Nazarov, Multi-terminal Josephson junctions as topological matter, *Nat. Commun.* **7**, 11167 (2016).
 - [32] L. Peralta Gavensky, G. Usaj, and C. A. Balseiro, Multiterminal Josephson junctions: A road to topological flux networks, *Europhys. Lett.* **141**, 36001 (2022).
 - [33] Z. Su, A. B. Tacla, M. Hocevar, D. Car, S. R. Plissard, E. P. A. M. Bakkers, A. J. Daley, D. Pekker, and S. M. Frolov, Andreev molecules in semiconductor nanowire double quantum dots, *Nat. Commun.* **8**, 585 (2017).
 - [34] J.-D. Pillet, V. Benzoni, J. Griesmar, J.-L. Smir, and Çağlar Ö. Girit, Scattering description of Andreev molecules, *SciPost Phys. Core* **2**, 009 (2020).
 - [35] K. Sakurai, M. T. Mercaldo, S. Kobayashi, A. Yamakage, S. Ikegaya, T. Habe, P. Kotetes, M. Cuoco, and Y. Asano, Nodal Andreev spectra in multi-Majorana three-terminal Josephson junctions, *Phys. Rev. B* **101**, 174506 (2020).
 - [36] S. Matsuo, T. Imoto, T. Yokoyama, Y. Sato, T. Lindemann, S. Gronin, G. C. Gardner, S. Nakosai, Y. Tanaka, M. J. Manfra, *et al.*, Phase-dependent Andreev molecules and superconducting gap closing in coherently-coupled Josephson junctions, *Nat. Commun.* **14**, 8271 (2023).
 - [37] M. Coraiola, D. Z. Haxell, D. Sabonis, H. Weisbrich, A. E. Svetogorov, M. Hinderling, S. C. ten Kate, E. Cheah, F. Krizek, R. Schott, W. Wegscheider, J. C. Cuevas, W. Belzig, and F. Nichele, Phase-engineering the Andreev band structure of a three-terminal Josephson junction, *Nat. Commun.* **14**, 6784 (2023).
 - [38] F. Matute-Cañadas, L. Tosi, and A. L. Yeyati, Quantum circuits with multiterminal Josephson-Andreev junctions, *PRX Quantum* **5**, 020340 (2024).
 - [39] J.-D. Pillet, V. Benzoni, J. Griesmar, J.-L. Smir, and c. O. Girit, Nonlocal Josephson effect in Andreev molecules, *Nano Letters* **19**, 7138 (2019).
 - [40] N. Pankratova, H. Lee, R. Kuzmin, K. Wickramasinghe, W. Mayer, J. Yuan, M. G. Vavilov, J. Shabani, and V. E.

- Manucharyan, Multiterminal Josephson effect, *Phys. Rev. X* **10**, 031051 (2020).
- [41] S. Matsuo, J. S. Lee, C.-Y. Chang, Y. Sato, K. Ueda, C. J. Palmström, and S. Tarucha, Observation of nonlocal Josephson effect on double InAs nanowires, *Commun. Phys.* **5**, 221 (2022).
- [42] S. Matsuo, T. Imoto, T. Yokoyama, Y. Sato, T. Lindemann, S. Gronin, G. C. Gardner, M. J. Manfra, and S. Tarucha, Phase engineering of anomalous Josephson effect derived from Andreev molecules, *Science Advances* **9**, eadj3698 (2023).
- [43] D. Z. Haxell, M. Coraiola, M. Hinderling, S. C. ten Kate, D. Sabonis, A. E. Svetogorov, W. Belzig, E. Cheah, F. Krizek, R. Schott, W. Wegscheider, and F. Nichele, Demonstration of the nonlocal Josephson effect in Andreev molecules, *Nano Letters* **23**, 7532 (2023).
- [44] J. Cayao, P. Buset, and Y. Tanaka, Controllable odd-frequency Cooper pairs in multiterminal superconductor Josephson junctions, *Phys. Rev. B* **109**, 205406 (2024).
- [45] J. H. Correa and M. P. Nowak, Theory of universal diode effect in three-terminal Josephson junctions, *SciPost Phys.* **17**, 037 (2024).
- [46] M. Tinkham, *Introduction to superconductivity* (Courier Corporation, 2004).
- [47] M. Leijnse and K. Flensberg, Parity qubits and poor man's Majorana bound states in double quantum dots, *Phys. Rev. B* **86**, 134528 (2012).
- [48] J. Cayao and R. Aguado, Non-Hermitian minimal Kitaev chains, *arXiv:2406.18974* (2024).
- [49] J. Cayao, Emergent pair symmetries in systems with poor man's Majorana modes, *Phys. Rev. B* **110**, 125408 (2024).
- [50] Y. Tanaka, S. Tamura, and J. Cayao, Theory of Majorana zero modes in unconventional superconductors, *Prog. Theor. Exp. Phys.*, ptae065 (2024).
- [51] K. Kawabata, T. Bessho, and M. Sato, Classification of exceptional points and non-Hermitian topological semimetals, *Phys. Rev. Lett.* **123**, 066405 (2019).
- [52] F. S. Bergeret, A. F. Volkov, and K. B. Efetov, Odd triplet superconductivity and related phenomena in superconductor-ferromagnet structures, *Rev. Mod. Phys.* **77**, 1321 (2005).
- [53] T. Dvir, G. Wang, N. van Loo, C.-X. Liu, G. P. Mazur, A. Bordin, S. L. Ten Haaf, J.-Y. Wang, D. van Driel, F. Zatelli, *et al.*, Realization of a minimal Kitaev chain in coupled quantum dots, *Nature* **614**, 445 (2023).
- [54] A. Bordin, X. Li, D. van Driel, J. C. Wolff, Q. Wang, S. L. D. ten Haaf, G. Wang, N. van Loo, L. P. Kouwenhoven, and T. Dvir, Crossed Andreev reflection and elastic co-tunneling in a three-site Kitaev chain nanowire device, *arXiv:2306.07696* (2023).
- [55] A. Bordin, G. Wang, C.-X. Liu, S. L. D. ten Haaf, N. van Loo, G. P. Mazur, D. Xu, D. van Driel, F. Zatelli, S. Gazibegovic, G. Badawy, E. P. A. M. Bakkers, M. Wimmer, L. P. Kouwenhoven, and T. Dvir, Tunable crossed Andreev reflection and elastic cotunneling in hybrid nanowires, *Phys. Rev. X* **13**, 031031 (2023).
- [56] F. Zatelli, D. van Driel, D. Xu, G. Wang, C.-X. Liu, A. Bordin, B. Roovers, G. P. Mazur, N. van Loo, J. C. Wolff, A. M. Bozkurt, G. Badawy, S. Gazibegovic, E. P. A. M. Bakkers, M. Wimmer, L. P. Kouwenhoven, and T. Dvir, Robust poor man's Majorana zero modes using Yu-Shiba-Rusinov states, *arXiv:2311.03193* (2023).
- [57] E. Strambini, S. D'ambrosio, F. Vischi, F. Bergeret, Y. V. Nazarov, and F. Giazotto, The ω -squipt as a tool to phase-engineer Josephson topological materials, *Nat. Nanotech.* **11**, 1055 (2016).
- [58] A. W. Draelos, M.-T. Wei, A. Seredinski, H. Li, Y. Mehta, K. Watanabe, T. Taniguchi, I. V. Borzenets, F. Amet, and G. Finkelstein, Supercurrent flow in multiterminal graphene Josephson junctions, *Nano Lett.* **19**, 1039 (2019).
- [59] G. V. Graziano, M. Gupta, M. Pendharkar, J. T. Dong, C. P. Dempsey, C. Palmström, and V. S. Pribiag, Selective control of conductance modes in multi-terminal Josephson junctions, *Nat. Commun.* **13**, 5933 (2022).
- [60] D. C. Ohnmacht, V. Wilhelm, H. Weisbrich, and W. Belzig, Non-hermitian topology in multiterminal superconducting junctions, *arXiv:2408.01289* (2024).